Harmonic elimination in a hysteresis-based direct torque Control of matrix converter-fed five-phase PMSM

Arjang Yousefi-Talouki* **S. Asghar Gholamian*** **Ahmad Radan****

*Babol University of Technology, Iran, +98-111-3239214, a.yousefi@stu.nit.ac.ir

** K.N.Toosi University of Technology, Tehran, Iran

***Abstract**: A novel direct torque control of matrix converter-fed five-phase permanent magnet synchronous motor (PMSM) is proposed in this paper. Due to some special applications of multiphase motors such as aerospace and ship propulsion, the volume and the weight of these drives are the most important challenging problems. Matrix converters allow a compact design due to lack of bulky dc-link capacitor and therefore can be reasonable alternatives to the conventional Voltage source inverters. Also, matrix converters generate higher number of output voltage vectors. As a consequence besides the control of electromagnetic torque and stator flux, input power factor can be controlled. In the reported direct torque control of five-phase PMSMs in the literatures, large harmonic current is a serious drawback. In this paper a new switching table is achieved that removes this problem. The novelty of this proposed method is characterized by simple structure, using matrix converter, large stator current harmonic elimination, unity input power factor and also torque ripple reduction.*

***Key words:** DTC, Five-Phase, PMSM, Matrix Converter, Harmonic Elimination*

1. Introduction

A great deal of research has been carried out over the past decades on multiphase motors due to their lots of advantages over their three-phase counterparts, such as reducing the amplitude of torque pulsations, lowering the dc link current harmonics, reducing the stator current per phase without increasing the voltage per phase and increasing the reliability [1-6].

Direct Torque Control (DTC) is one of the active researched control schemes which is based on the decoupled control of flux and toque. The basic principle of DTC is to directly select stator voltage vectors according to the differences between the reference and actual torque and stator flux linkage. DTC provides a very quick and precise torque response and also has very simple instruction, i.e., no need of rotary coordinate transformation, inner current regulator, or pulse width modulation (PWM) block. This method was first proposed for three-phase induction machines and then was implemented on three-phase permanent magnet synchronous motors (PMSMs) [7-8]. Space vector modulation (SVM)-based DTC methods have been presented in order to torque ripple reduction and achieving constant switching frequency [9-12]. But, it should be noted that DTC-SVM methods looses the simplicity of hysteresis-based DTC methods. Also, DTC method was presented for the first time in five and six-phase induction motors in [13-14]. L. Parsa, et al. investigated the DTC algorithm for a five-phase PMSM in [15].

In a five-phase system, all the five-phase variables can be transferred in to two vector planes, $d-q$ and z_1-z_2. The harmonics with the orders of $10n\pm1$(n is an integer) with the abcde phase sequence are related to $d-q$ plane and the harmonics with the orders of $10n\pm3$(n is an integer) with the acebd phase sequence are related to z_1-z_2 plane. It is seen in [15] that, when a voltage vector in $d-q$ plane is energized, it's correspond vector in z_1-z_2 plane, also is energized, simultaneously. Therefore, unwanted harmonic voltages with the orders of $10n\pm3$ are obtained and hence large harmonic currents are generated. As a consequence, it can be said that the literature [15] has a serious drawback. High current distortion is achieved in this method because the low-frequency current space vectors in auxiliary vector sub-space are not eliminated. Thus, third

and seventh harmonic orders are remarkable in this presented scheme. Some literatures proposed space vector modulation (SVM) method to eliminate harmonic problems [16-18]. But, these methods have complicated structures and calculations. The authors of [19] presented a new scheme to overcome harmonic problem. This method uses ten virtual vectors which each voltage vector is composed of large and medium vectors of $d-q$ plane.

Electrical and hybrid vehicles, aerospace, ship propulsion and wind power applications are some examples where multiphase drives can be used [1-6]. In all of these industrial areas, the volume of motor-drive package is an important problem. However, in the most of reported literatures, voltage source inverter (VSI)-fed multiphase-motor drives have been investigated which have huge electrolyte capacitors in their dc-link. On the other hand, these capacitors reduce the reliability of such motor drives. Matrix converters (MCs) as ac-ac converters have emerged to become an attractive alternative to the conventional converters [20-22]. MCs hold many advantages, including an adjustable input power factor, bidirectional power flow, high-quality power output waveforms and the lack of bulky capacitors. These converters produce higher number of voltage space vectors in comparison with conventional VSIs. Thus, moreover the precise control on torque and flux, also the control of input power factor can be done using degrees of freedom of MC. Direct torque control method using matrix converter was implemented on induction motor and PMSMs [23-24]. It is shown that by using matrix converter, a precise torque and flux control and also unity input power factor will be achieved. Despite of more advantages of MCs in comparison with conventional VSIs, in the literatures related to the five-phase motor drives, only VSIs have been used to feed these motors.

This paper proposes a new switching-table direct torque control of five-phase PMSMs using MCs. In this presented scheme, the problem of large harmonic currents is eliminated which is the most drawbacks of DTC of five-phase motors. The principle of this method is based on that of method reported in [19]. Using MC, close-to-unity input power factor is achievable and also good control in torque and flux is obtained. Due to compact designs of MC, this method allows a lower weight dive in comparison with classic ones. In the other word, the advantages of DTC method and MCs are combined in this presented scheme.

2. Five-Phase PMSM Equations

The stator voltage equation of the motor is as follow [15]:

$$V_s = R_s I_s + \frac{d\Lambda_s}{dt} \tag{1}$$

R_s, I_s and Λ_s are the stator resistance, current and flux linkage matrices, respectively.

The equation of air gap flux linkage can be presented as follow:

$$\Lambda_s = \Lambda_{ss} + \Lambda_m = L_{ss} I_s + \Lambda_m \tag{2}$$

L_{ss} is the stator inductance matrix and Λ_m is the flux linkage of the rotor permanent magnet.

One can write the stator voltage, flux and torque equations of a five-phase sinusoidal wounded motor in synchronous rotating reference frame ($d-q-z_1-z_2-z_3$) using the following transformation matrix.

$$T(\theta)=\frac{2}{5}\begin{bmatrix} \cos(\theta) & \cos(\theta-\frac{2\pi}{5}) & \cos(\theta-\frac{4\pi}{5}) & \cos(\theta+\frac{4\pi}{5}) & \cos(\theta+\frac{2\pi}{5}) \\ \sin(\theta) & \sin(\theta-\frac{2\pi}{5}) & \sin(\theta-\frac{4\pi}{5}) & \sin(\theta+\frac{4\pi}{5}) & \sin(\theta+\frac{2\pi}{5}) \\ \cos(\theta) & \cos(\theta+\frac{4\pi}{5}) & \sin(\theta-\frac{2\pi}{5}) & \cos(\theta+\frac{2\pi}{5}) & \cos(\theta-\frac{4\pi}{5}) \\ \sin(\theta) & \sin(\theta+\frac{4\pi}{5}) & \sin(\theta-\frac{2\pi}{5}) & \sin(\theta+\frac{2\pi}{5}) & \sin(\theta-\frac{4\pi}{5}) \\ \frac{1}{\sqrt{2}} & \frac{1}{\sqrt{2}} & \frac{1}{\sqrt{2}} & \frac{1}{\sqrt{2}} & \frac{1}{\sqrt{2}} \end{bmatrix} \tag{3}$$

In the above equation, θ is the rotor electrical angle.

Stator voltage equations in synchronous reference frame are obtained as

$$\begin{aligned} V_{qs} &= r_s i_{qs} + \omega\lambda_{ds} + \frac{d\lambda_{qs}}{dt} \\ V_{ds} &= r_s i_{ds} - \omega\lambda_{qs} + \frac{d\lambda_{ds}}{dt} \\ V_{z1s} &= r_s i_{z1s} + \frac{d\lambda_{z1s}}{dt} \\ V_{z2s} &= r_s i_{z2s} + \frac{d\lambda_{z2s}}{dt} \end{aligned} \tag{4}$$

Where, ω is the rotor electrical speed.

The stator flux linkages are given by

$$\lambda_{ds} = L_d i_{ds} + \lambda_m$$
$$\lambda_{qs} = L_q i_{qs}$$
$$\lambda_{z1s} = L_{ls} i_{z1s} \quad (5)$$
$$\lambda_{z2s} = L_{ls} i_{z2s}$$
$$\lambda_{z3s} = L_{ls} i_{z3s}$$

All the 10n±1th (n=0,1,2…) winding space harmonics and voltage time harmonics with abcde phase sequence are related to $d-q$ subspace, while all the 10n±3th (n=0,1,2…) winding space harmonics and voltage time harmonics with acebd phase sequence are related to $Z_1 - Z_2$ subspace. For a sinusoidal wounded motor, magnitude of third space harmonic within stator winding function is very low, which leads to tiny magnetizing inductance in $Z_1 - Z_2$ model and therefore the only impedance to $Z_1 - Z_2$ voltage is stator resistance in series with stator leakage inductance, as can be seen in (4). As a consequence, low-order voltage harmonic in $Z_1 - Z_2$ plane, cause to large distortion in stator current [15].

Electromagnetic torque equation can be written as follow:

$$T_e = \frac{p}{2}\frac{5}{2}[\lambda_m i_{qs} + (L_d - L_q) i_{ds} i_{qs}] \quad (6)$$

As can be seen in (6), only the components of $d-q$ subspace contribute to electromagnetic torque. Therefore, increasing or decreasing the load torque doesn't influence on the magnitude of currents in $z_1 - z_2$ vector plane and hence the magnitude of harmonics with the orders of ($10n \pm 3$) is constant regardless to the load torque.

3. Direct torque control of five-phase PMSM

DTC of VSI-fed five-phase PMSMs is reported in detail in [15]. A five-phase VSI produce 32 output voltage vectors consisting of 30 active and two zero voltage vectors. Fig.1 shows the voltage vectors of a five-phase VSI in both $d-q$ and $z_1 - z_2$ subspaces. The following properties can be summarized from this figure:

1) The ratio of the amplitudes of voltage vectors is $1:1.618:1.618^2$ from the small vectors to large vectors.
2) The outer decagon of the $d-q$ subspace is mapped into the inner decagon of the $z_1 - z_2$ subspace and vice-versa. The medium decagon of $d-q$ is mapped into the medium decagon of $z_1 - z_2$. In the other word, when a voltage vector of $d-q$ plane is energized, its corresponding voltage vector in $z_1 - z_2$ plane is also energized simultaneously.

Referring to (6), it is concluded that electromagnetic torque is only dependant to components of $d-q$ vector plane. Therefore, the selection of appropriate voltage vectors is based on the position of stator flux position in $d-q$ plane. It is seen in Fig.1 that the switching pattern plane is divided to ten sectors. According to stator flux position, torque and flux hysteresis controller outputs, the authors of [15] derived a switching table.

However, this presented DTC scheme has a serious drawback. As mentioned earlier, when a voltage vector of $d-q$ plane is energized, its corresponding voltage vector in $z_1 - z_2$ plane is energized simultaneously and also it has been explained that the harmonic variables with the orders of $(10n \pm 3)$ are related to $z_1 - z_2$ plane. Therefore, there are low-order voltage harmonics (as example third and seventh) which generate huge harmonic currents.

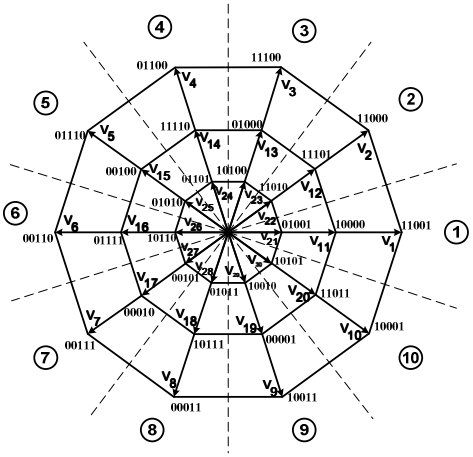

$d-q$ Plane

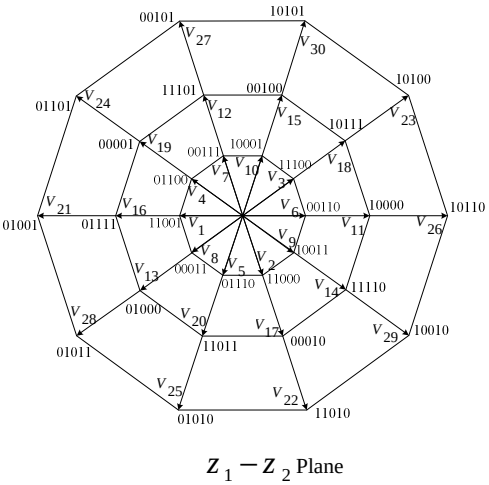

$z_1 - z_2$ Plane

Fig.1. thirty two voltage vectors of a five-phase VSI

4. Proposed DTC

4.1. Three-phase to five-phase matrix converter

A schematic diagram of a three-phase to five-phase matrix converter is shown in Fig.2. As can be seen, there are five legs which each leg have three bidirectional switches in series. Each bidirectional switch is composed of two IGBTs and two fast diodes connected anti-parallel. Each switch has a switching function which is defined as follows. In the following equation, j and k represent input and output phases, respectively.

$$S_{jk}(t) = \begin{cases} 0 & \text{switch, } S_{jk} \text{ is open} \\ 1 & \text{switch, } S_{jk} \text{ is closed} \end{cases} \qquad (7)$$
$$j = \{A,B,C\}, \quad k = \{a,b,c,d,e\}$$

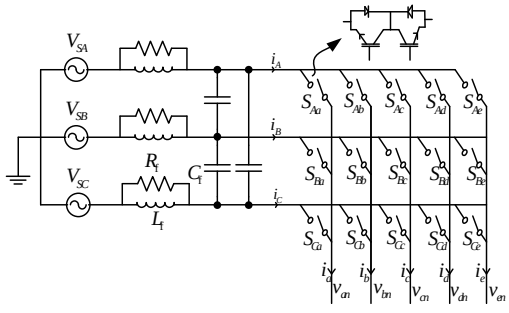

Fig.2. Schematic diagram of three-phase to five-phase MC

As three-phase MCs, in a five-phase MC any two input terminals shouldn't be connected to the same output phase to prevent short circuit. On the other hand, an output phase must never be open circuited, because there is no path for the inductive load current which leads to over voltages.

The space vector representation of voltages and currents are as follows:

$$V_o^{d-q} = \frac{2}{5}(V_a + V_b e^{j\frac{2\pi}{5}} + V_c e^{j\frac{4\pi}{5}} + V_d e^{-j\frac{4\pi}{5}} + V_e e^{-j\frac{2\pi}{5}}) = V_o e^{j\alpha_o} \qquad (8)$$

$$V_o^{z_1-z_2} = \frac{2}{5}(V_a + V_b e^{-j\frac{4\pi}{5}} + V_c e^{j\frac{2\pi}{5}} + V_d e^{-j\frac{2\pi}{5}} + V_e e^{j\frac{4\pi}{5}}) = V_o e^{j\alpha_o} \qquad (9)$$

$$i_i = \frac{2}{3}(i_A + i_B e^{j\frac{2\pi}{3}} + i_C e^{-j\frac{2\pi}{3}}) = i_i e^{j\beta_i} \qquad (10)$$

A three-phase to five-phase MC produce $3^5 = 243$ output voltage space vectors. Among these vectors, 93 vectors so-called stationary vectors have fixed direction. In the case of five-phase matrix converters, as well as five-phase VSIs, the output vectors form three concentric decagons, so that, 30 output voltage space vectors are large vectors, 30 vectors are medium and the last 30 vectors are small vectors. It should be noted that three vectors are zero voltage space vectors. These 93 vectors consist of four configurations.

1) (Large vectors): In the first configuration 3 adjacent output phases are connected to the same input phase and the 2 other output phases are connected to another input phase. For example, output phases of "a", "b" and "c" are connected to input phase of "A", and both of output phases of "d" and "e" are connected to input phase of "B". These switching configurations consist of 30 output voltage vectors. These vectors are summarized in table.A.1 in Appendix.
2) (Medium vectors): In the second configuration, 4 of the output phases are connected to the same input phase and the fifth output phase is connected to any other input phase. For example, output phases of "a", "b", "c" and "d" are connected to input phase of "A" and the

last output phase, “e”, is connected to input phase of “B”. These switching configurations consist of 30 output voltage vectors. These vectors are summarized in table.A.2 in Appendix.

3) (Small vectors): In the third configuration 3 alternate output phases are connected to the same input phase and the 2 other output phases are connected to another input phase. For example, output phases of “a”, “b” and “d” are connected to input phase of “A”, and both of output phases of “c” and “e” are connected to input phase of “B”. These switching configurations consist of 30 output voltage vectors These vectors are summarized in table.A.3 in Appendix.
4) (Zero vectors): In the fourth configuration, all of output phases are connected to a same input phase. In these configurations zero voltage vectors are produced. It is notable that 3 zero vectors are achieved.

Fig.3 illustrates the output line-to-neutral voltage vector and the input line current vector configurations.

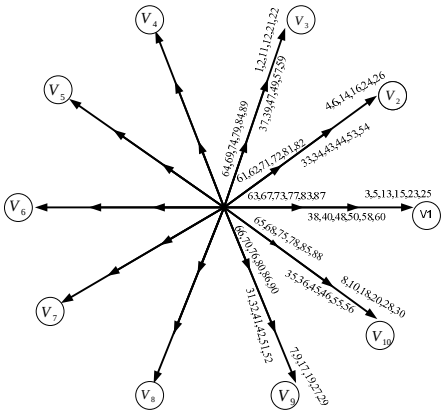

(a)

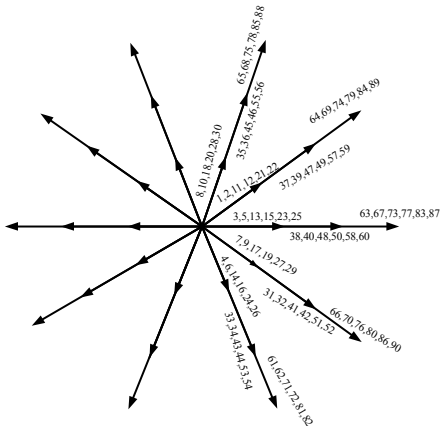

(b)

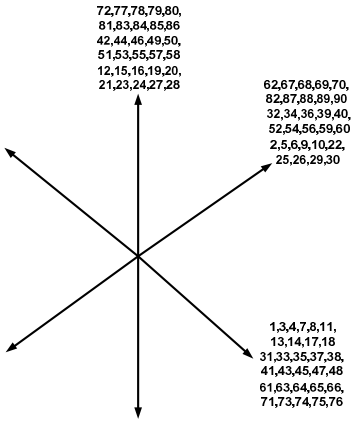

(C)

Fig.3. a) output line-to-neutral voltage vector configurations in d-q plane, b) output line-to-neutral voltage vector configurations in z1-z2 plane, c) line current vector configurations

4.2. DTC of five-phase PMSM using matrix converter

From previous considerations, it appears that the magnitude of output voltage vectors of matrix converter is related to the line-to-line input voltages. The path of input voltages is shown in Fig.4. As can be seen, the input voltages path is divided to six sectors starting at $-\pi/6 rad$ in sector one. Also, in each sector there are four voltages with large amplitudes and two voltages with small ones. The small vectors cannot be used in DTC method due to their change of sign in the middle of the sector. In Fig.3, voltage vectors $v_1 - v_{10}$ show the matrix converter vectors as the same direction as those vectors delivered by VSIs. The criteria to implement a switching table for matrix converter can be explained using an example. It is

considered that V_1 is the VSI output voltage vector in a conventional DTC. From Fig.3 (a) and table.A.1, it appears that voltage vectors (3, 5, 13, 15, 23 and 25) must be chosen. If the input line-to-neutral voltage lies in sector 1, the switching configurations which can be utilized are 3 and 5. The reason of not choosing the four other vectors is that, vectors 15 and 23 are related to the small line-to-line voltage vectors in sector 1 (V_{bc} or V_{cb}) and cannot be used. Vectors 13 and 25 are in the opposite direction of V_1 and therefore cannot be used. Vector 3 and 5 impose two input current vectors with different directions, as shown in Fig.3 (c). Thus, this degree of freedom can be used for controlling the average value of the sine of the displacement angle φ between input voltage vector and input current vector. If $\sin(\psi) = 0$, unity input power factor is achieved. Therefore, under control process, the reference value of $\sin(\psi)$ is set to be zero. If the average value of $\sin(\psi)$ needs to be decreased, voltage vector 5 should be chosen. On the contrary, if the average value of $\sin(\psi)$ has to be increased, voltage vector 3 has to be applied. According to these discussed principles, a new switching table is arranged which can be seen in table.1. The first column is related to the output voltage vectors selected by the conventional DTC. The other 6 columns contain the sectors which the input line-to-neutral voltage vectors lie in. If the average value of $\sin(\psi)$ needs to be increased (decreased) the right (left) sub-column is chosen. The block diagram of proposed DTC method is shown in Fig.5. In comparison with classical DTC, in this scheme one more hysteresis controller is needed in order to control $\sin(\psi)$. Also, the position of input voltage should be known in each sampling period of time.

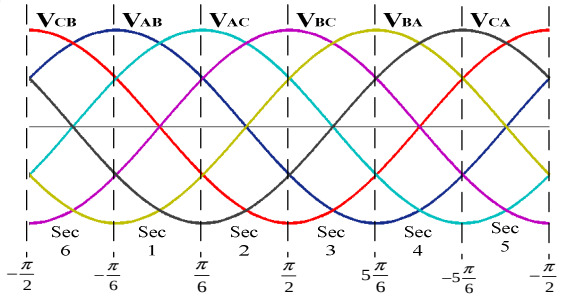

Fig.4. six sectors of input voltage vectors

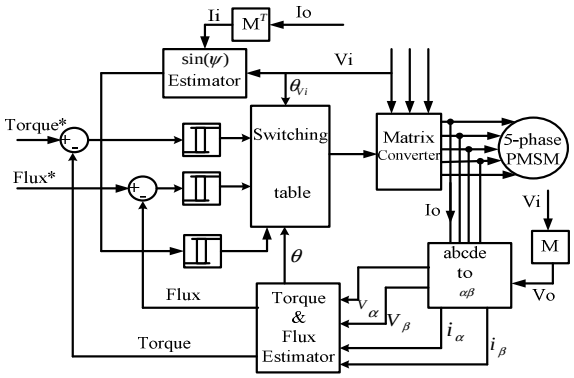

Fig.5. Schematic diagram of proposed DTC using matrix converter

TABLE 1. PROPOSED VOLTAGE VECTOR SWITCHING TABLE FOR MATRIX CONVERTER-FED FIVE-PHASE PMSM

	Sec 1		Sec 2		Sec 3		Sec 4		Sec 5		Sec 6	
	+1	-1	+1	-1	+1	-1	+1	-1	+1	-1	+1	-1
V1	5	3	15	5	13	15	25	13	23	25	3	23
V2	6	4	16	6	14	16	26	14	24	26	4	24
V3	2	1	12	2	11	12	22	11	21	22	1	21
V4	29	17	27	29	7	27	9	7	19	9	17	19
V5	30	18	28	30	8	28	10	8	20	10	18	20
V6	25	13	23	25	3	23	5	3	15	5	13	15
V7	26	14	24	26	4	24	6	4	16	6	14	16
V8	22	11	21	22	1	21	2	1	12	2	11	12
V9	9	7	19	9	17	19	29	17	27	29	7	27
V10	10	8	20	10	18	20	30	18	28	30	8	28

4.3. Harmonic currents Elimination

As previously explained in both classical and proposed DTC, a voltage vector of $d-q$ plane is selected in a sampling period of time T_s. Therefore, a voltage vector of $z_1 - z_2$ plane is energized simultaneously which leads to harmonic currents. On the other hand, if the switching configuration is such a way that the magnitude of $z_1 - z_2$ axes voltage vector is zero, the harmonics are eliminated and sinusoidal output voltage is achieved.

Referring to Fig.1, it is seen that, aligned large and medium vectors in $d-q$ vector plane, produce small and medium vectors in opposite direction in $z_1 - z_2$ plane. For example, voltage vectors V_2 and V_{12} have the same direction in

$d-q$ plane and opposite direction in z_1-z_2 plane. Since the ratio of the amplitudes of medium and small voltage vectors in z_1-z_2 plane are 1.618, the dwell time of 1.618 between these two voltage vectors in a sampling time, will produce zero-mean volt-second in z_1-z_2 plane [19]. In the other word, if the "on-state time" of voltage vector V_2 is set such a way that to be 1.618 times bigger than the "on-state time" of voltage vectorV_{12}, a zero-mean volt-second will be produced in z_1-z_2 plane.

As same as VSI vectors, in the case of MC, referring to Fig.3, table.A.1 and table.A.2, it is seen that medium voltage vectors V_{38} andV_{40} have the same directions with the large vectors V_3 andV_5, respectively. On the other hand, it is seen in Fig.3 (b) that voltage vectors V_3 and V_{38} or vectors V_5 andV_{40}, have the opposite direction in z_1-z_2 plane.

The criteria to achieve a switching table can be explained with the following example. It is assumed that, the input line-to-neutral voltage lies in sector 1 and the output voltage vector of conventional DTC in a period of sampling time is vectorV_1. It has been shown in table.2 that for this situation, large voltage vectors 3 and 5 can be used. Therefore, in a predefined sampling time the proposed switching configurations between vectors 3 and 38 or vectors 5 and 40, "such as shown in Fig.6", will produce zero-mean volt-second in z_1-z_2 plane.

According to mentioned explanations, a switching table is derived which is summarized in table.2. It should be noted that, the symbol of V_i^j in this table means the combination of large vectorV_i and medium vectorV_j which are in the same direction in$d-q$ vector plane.

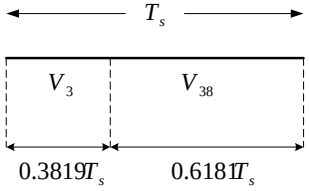

Fig.6. switching state between vectors 3 and 38 in a sample time

TABLE 2. PROPOSED SWITCHING TABLE FOR MATRIX CONVERTER-FED FIVE-PHASE PMSM IN ORDER TO HARMONIC ELIMINATION

	Sec 1		Sec 2		Sec 3		Sec 4		Sec 5		Sec 6	
	+1	-1	+1	-1	+1	-1	+1	-1	+1	-1	+1	-1
V1	V_5^{40}	V_3^{38}	V_{15}^{50}	V_5^{40}	V_{13}^{48}	V_{15}^{50}	V_{25}^{60}	V_{13}^{48}	V_{23}^{58}	V_{25}^{60}	V_3^{38}	V_{23}^{58}
V2	V_6^{34}	V_4^{33}	V_{16}^{44}	V_6^{34}	V_{14}^{43}	V_{16}^{44}	V_{26}^{54}	V_{14}^{43}	V_{24}^{53}	V_{26}^{54}	V_4^{33}	V_{24}^{53}
V3	V_2^{59}	V_1^{47}	V_{12}^{57}	V_2^{59}	V_{11}^{37}	V_{12}^{57}	V_{22}^{39}	V_{11}^{37}	V_{21}^{49}	V_{22}^{39}	V_1^{47}	V_{21}^{49}
V4	V_{29}^{32}	V_{17}^{31}	V_{27}^{42}	V_{29}^{32}	V_7^{41}	V_{27}^{42}	V_9^{52}	V_7^{41}	V_{19}^{51}	V_9^{52}	V_{17}^{31}	V_{19}^{51}
V5	V_{30}^{56}	V_{18}^{45}	V_{28}^{55}	V_{30}^{56}	V_8^{35}	V_{28}^{55}	V_{10}^{36}	V_8^{35}	V_{20}^{46}	V_{10}^{36}	V_{18}^{45}	V_{20}^{46}
V6	V_{25}^{60}	V_{13}^{48}	V_{23}^{58}	V_{25}^{60}	V_3^{38}	V_{23}^{58}	V_5^{40}	V_3^{38}	V_{15}^{50}	V_5^{40}	V_{13}^{48}	V_{15}^{50}
V7	V_{26}^{54}	V_{14}^{43}	V_{24}^{53}	V_{26}^{54}	V_4^{33}	V_{24}^{53}	V_6^{34}	V_4^{33}	V_{16}^{44}	V_6^{34}	V_{14}^{43}	V_{16}^{44}
V8	V_{22}^{39}	V_{11}^{37}	V_{21}^{49}	V_{22}^{39}	V_1^{47}	V_{21}^{49}	V_2^{59}	V_1^{47}	V_{12}^{57}	V_2^{59}	V_{11}^{37}	V_{12}^{57}
V9	V_9^{52}	V_7^{41}	V_{19}^{51}	V_9^{52}	V_{17}^{31}	V_{19}^{51}	V_{29}^{32}	V_{17}^{31}	V_{27}^{42}	V_{29}^{32}	V_7^{41}	V_{27}^{42}
V10	V_{10}^{36}	V_8^{35}	V_{20}^{46}	V_{10}^{36}	V_{18}^{45}	V_{20}^{46}	V_{30}^{56}	V_{18}^{45}	V_{28}^{55}	V_{30}^{56}	V_8^{35}	V_{28}^{55}

5. Simulation Results

Simulations have been performed on Matlab/Simulink to verify the feasibility of the proposed method. The drive has been tested in various steady state and dynamic performances. The parameters of test machines are given in table.3.

TABLE 3. THE PARAMETERS OF FIVE-PHASE PMSM

P(poles)	Ld	Lq	Rs	J	B	ψ_f
4	18 mh	42mH	0.7 Ω	0.025	0.005	0.5 (Wb)

5.1. Steady-State Behavior

The steady state behavior of the drive is studied at the rotor speed of 1000 r/min and load torque of 15 N.m. Fig.7 shows the electromagnetic torque waveforms for classical and proposed DTC. It shown that as well as classical DTC, electromagnetic torque tracks its reference very well. As expected, it is seen that the torque ripple in proposed DTC is reduced with respect to classical one, because large and medium decagon of voltage vectors are used in this method.

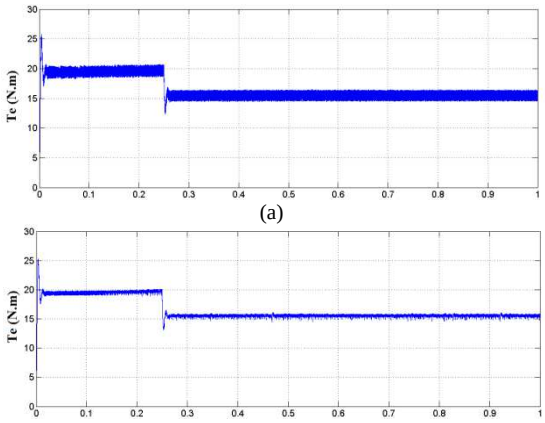

(a)

(b)

Fig.7. electromagnetic torque: a) classical DTC, b) proposed DTC

The stator flux in $\alpha-$axes and $\beta-$axes versus time is shown in Fig.8. As it can be observed, stator flux follows its reference value (0.5 Wb) very well.

The stator current is shown in Fig.9. As can be seen for classical DTC, the content of harmonic currents with the orders of 3 and 7 is high. From Fig.9 (b) it is concluded that large harmonic currents are eliminated in proposed DTC. Total harmonic distortion (THD) of stator current is illustrated in Fig.10. In classical DTC, THD is equal to 46.19%. It can be seen from Fig.10 (b) that, THD is completely reduced and is equal to 0.88% in proposed algorithm.

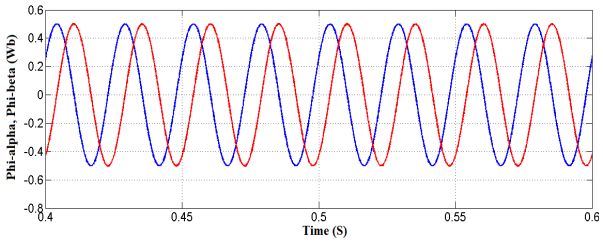

Fig.8. Stator flux, in α – axes and β – axes versus time

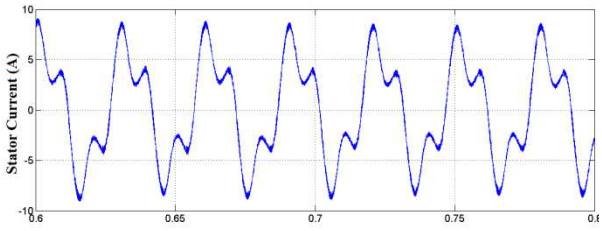

(a)

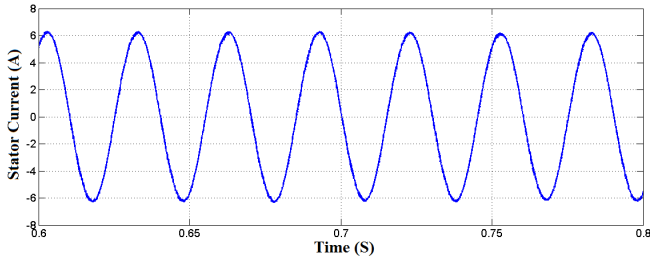

(b)

Fig.9. Stator current: a) classical, b) proposed DTC

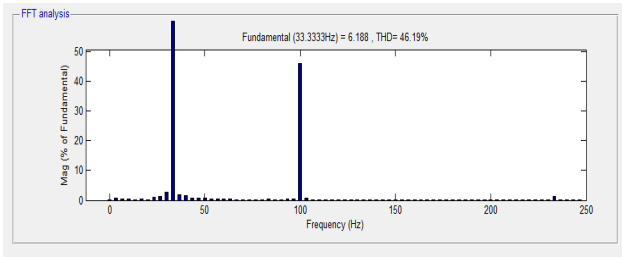

(a)

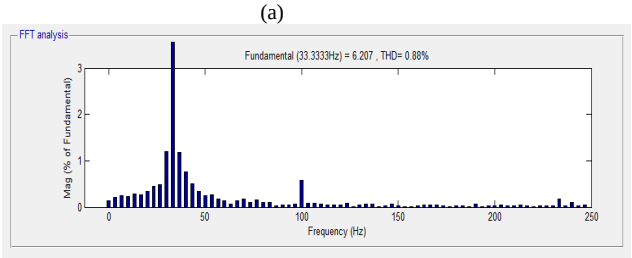

(b)

Fig.10. Comparison of harmonic spectra: a) classical DTC, b) proposed DTC

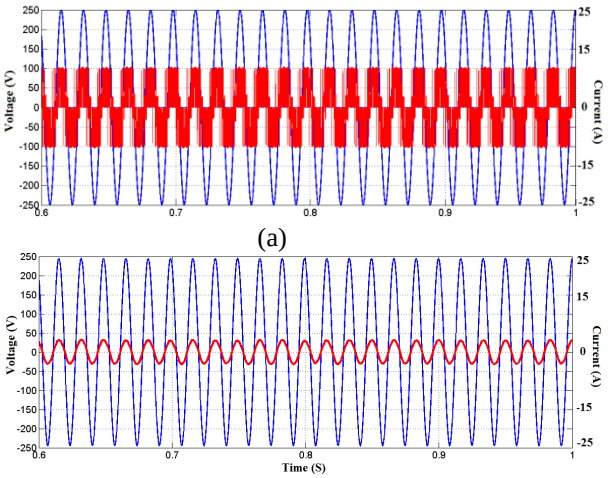

(a)

(b)

Fig.11. Line-to-neutral input voltage (phase-a) and its corresponding line current: a) unfiltered current, b) filtered current

Fig11 shows the input line-to-neutral voltage and its corresponding line current. As can be

seen in Fig.11 (a), the unfiltered input line current is in phase with its corresponding input phase voltage. Thus, close to unity input power factor is obtained in this presented method. The filtered input current and its corresponding voltage are illustrated in Fig.11 (b).

In the next step, the proposed drive performance is tested at low speeds. The rotor speed is considered to be 200 (r/min) and the load torque is 15 (N.m). As can be seen in Fig.12, electromagnetic torque follows its reference very well. Fig.13 shows the stator current. As well as stator current at high speeds, sinusoidal stator current is achieved at the speed of 200 r/min.

In the no-load condition and the rotor speed of 1200 r/min, stator current in classical DTC and proposed DTC is shown in Fig.14 (a) and Fig.14 (b), respectively. As it is seen, the content of third harmonic current is very high in classical DTC. It has been mentioned that the output torque of five-phase PMSM is only related to the components of $d-q$ vector plane. Therefore, increasing or decreasing the load torque and hence output electromagnetic torque doesn't influence on the components of z_1-z_2 vector plane. As a consequence, the magnitude of third harmonic current is constant in classical DTC. It is seen in this figure that, the magnitude of stator current at no-load condition is 3 (A) in classical DTC and 0.3 (A) in proposed DTC.

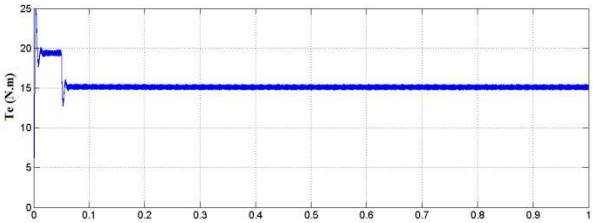

Fig.12. Electromagnetic torque waveform at the rotor speed of 200 r/min

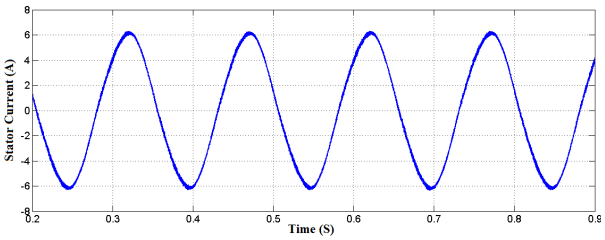

Fig.13. Stator current waveform at the rotor speed of 200 r/min

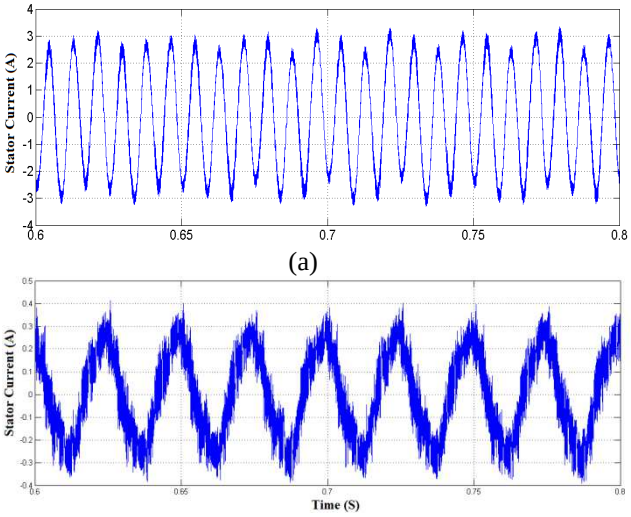

(a)

(b)

Fig.14. Stator current (phase-a) at 1200 r/min: a) classical DTC, b) proposed DTC

5.2. Dynamic Behavior

The dynamic behavior of the proposed drive is tested applying a step change load to the motor at the rotor speed of 1000 r/min. Referring to Fig.14 it is seen that due to use of combination of large and medium vectors, the torque ripple is clearly reduced in comparison with classical DTC. Also it is seen that electromagnetic torque follows its reference as well as classic DTC. The input phase voltage and its corresponding line current are shown in Fig.15 (a) to Fig.15 (d). It is seen that, from t=0.4 s to t=0.5 s, the input phase voltage and line current are in phase. From t=0.5 s to t=0.8 s, the input phase voltage and its corresponding line current are in the opposite phase due to regenerative mode of motor operation in this period of time. After t=0.8 s, the input phase voltage and input line current become in phase.

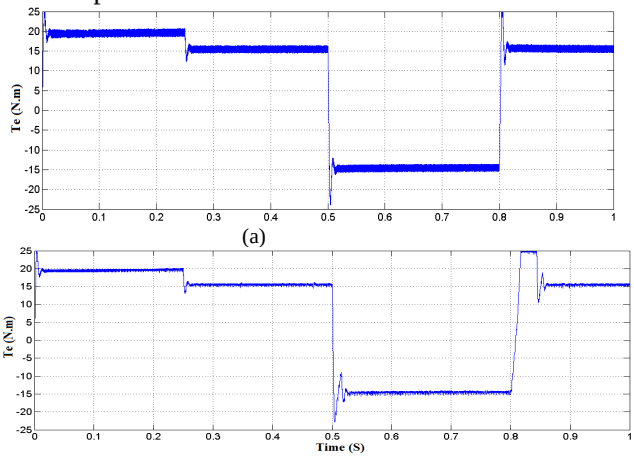

(a)

(b)

Fig.15. Electromagnetic torque waveform, a) classical DTC, b) Proposed DTC

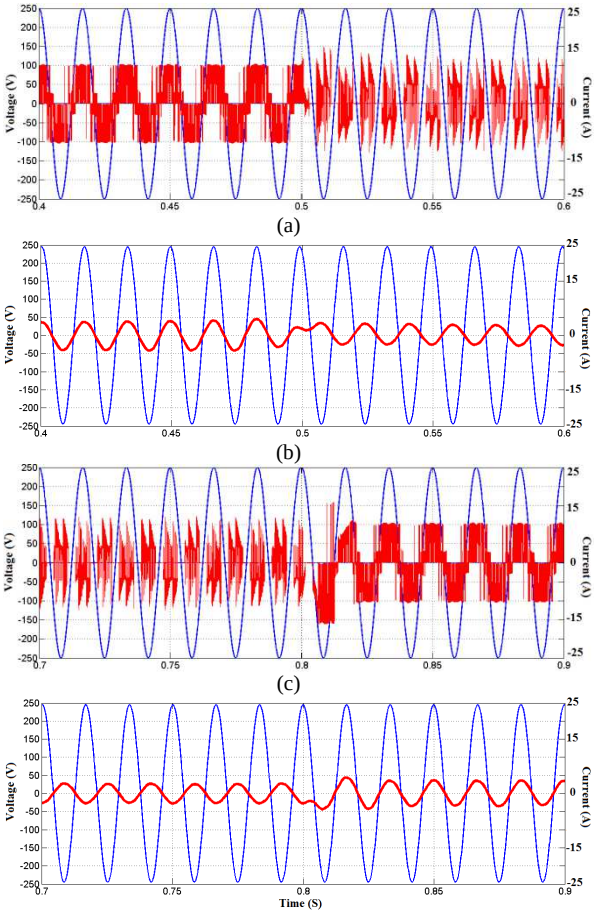

Fig.16. Line-to-neutral input voltage (phase-a) and its corresponding line current, a) unfiltered current from t=0.4 s to t=0.6 s, b) filtered current from t=0.4 s to t=0.6 s, c) unfiltered current from t=0.7 s to t=0.9 s, d) filtered current from t=0.7 s to t=0.9 s

6. Conclusion

A new hysteresis-based direct torque control of matrix converter-def five-phase PMSM has been presented in paper. Using a new switching table, the problem of large harmonic currents of these drives has been eliminated. All of the output voltage vectors of a three-phase to five-phase matrix converter have been extracted. Due to higher number of output voltage vectors in comparison with conventional VSIs, moreover the control of electromagnetic torque and stator flux, unity input power factor has been achieved. Simulation results verified the feasibility of proposed drive.

Appendix

The three Tables (A.1, A.2 and A.3), have been shown at the end of the paper after references.

References

1. L. Parsa, H.A. Toliyat, Fault-tolerant interior-permanent-magnet machines for hybrid electric vehicle applications, IEEE transaction on Vehicular Technology 56 (2007) 1546–1552.
2. E. Levi, R. Bojoi, F. Profumo, H.A. Toliyat, S. Williamson, Multiphase induction motor drives—a technology status review, IET- Electric Power Applications 1 (2007) 489–516.
3. L. Parsa, H.A. Toliyat, Five-phase permanent-magnet motor drives, IEEE transaction on Industry Applications 41 (2005) 30-37.
4. L. Guo, L. Parsa, Model reference adaptive control of five-phase IPM motors based on neural network, IEEE transaction on Industrial Electronics 59 (2012) 1500-1508.
5. A, Taheri, A. Rahmati, S. Kaboli, Efficiency improved in DTC of six-phase induction machine by adaptive gradient descent of flux, IEEE transaction on Power Electronics 27 (2012) 1552-1562.
6. M. Riswan Khan, A. Iqbal, Extended kalman filter based speeds estimation of series-connected five-phase two-motor drive system, Elsevier- Simulation Modelling Practice and Theory 17 (2009) 1346-1360.
7. L. Takahashi, T. Noguchi, A new quick-response and high-efficiency control strategy of an induction motor, IEEE transaction on Industry Applications IA-22 (1986) 820-827.
8. L. Zhong, M.F. Rahman, K.W. Lim, Analysis of Direct Torque Control in Permanent Magnet Synchronous Motor Drives, IEEE transaction on Power Electronics 12 (1997) 528-536.
9. Y.S. Lai, J.H. Chen, A new approach to direct torque control of induction motor drive for constant inverter switching frequency and torque ripple reduction, IEEE transaction on Energy Conversion 16 (2001) 220-227.
10. A. Tripathi, A.M. Khambadkone, S.K. Panda, Torque ripple analysis and dynamic performance of a space vector modulation based control method for ac-drives, IEEE transaction on Power Electronic 20 (2005) 485-492.
11. Y. Zhang, J. Zhu, W. Xu, Y. Guo, A simple method to reduce torque ripple in direct torque-controlled permanent-magnet synchronous motor by using vectors with variable amplitude and angle, IEEE transaction on Industrial Electronics 58 (2011) 2848-2859.
12. Z. Zhang, R. Tang, B. Bai, D. Xie, Novel direct torque control based on space vector modulation with adaptive stator flux observer for induction motors, IEEE Transaction on Magnetics 46 (2010) 3133-3136.
13. H.A. Toliyat, H. Xu, A novel direct torque control (DTC) method for five-phase induction machines, In: Proceedings of IEEE- Fifteenth annual IEEE applied power electronics conference and exposition (APEC), vol. 2; 2000.
14. R. Bojoi, F. Farina, G. Griva, F. Profumo, A. Tenconi, Direct torque control for dual three-phase induction motor drives, IEEE transaction on Industrial Applications 41 (2005) 627–1636.
15. L. Parsa, H.A. Toliyat, Sensorless direct torque control of five-phase interior permanent-magnet motor drives, IEEE transaction on Industrial Applications 43 (2007) 952–959.

16. P.S.N. de Silva, J.E. Fletcher, B.W. Williams, Development of space vector modulation strategies for five-phase voltage source inverters, Proceedings of IEE PEMD (2004) 650-655.
17. A. Iqbal, E. Levi, Space vector PWM techniques for sinusoidal output voltage generation with a five-phase voltage source inverter, Taylor & Francis- Electric Power Components and Systems 34 (2006) 119-140.
18. A. Iqbal, SK. Moinuddin, comprehensive relationship between carrier-based PWM and space vector PWM in a five-phase VSI, IEEE transaction on Circuit System 24 (2009) 2379-2390.
19. L. Zheng, J.E. Fletcher, B.W. Williams, X. He, A novel direct torque control scheme for a sensorless five-phase induction motor drive, IEEE transaction on Industrial Electronics 58 (2011) 503-513.
20. H. Carasa, R. Akkaya, Modelling and simulation of matrix converter under distorted input voltage conditions, Elsevier-Simulation Modelling Practice and Theory 19 (2011) 673-684.
21. P. Wheeler, J. Rodriguez, J. Clare, L. Empringham, A. Weinstein, Matrix converters: A technology review, IEEE transaction on Industrial Electronics 49 (2002) 276–288.
22. P. Wheeler, J. Clare, M. Apap, K.J. Bradley, Harmonic loss due to operation of induction machines from matrix converters, IEEE transaction on Industrial Electronics 55 (2008) 809–816.
23. D. Casadei, G.Serra, A. Tani, The use of matrix converters in direct torque control of induction machines, IEEE transaction on Industrial Electronics 48 (2001) 1057–1064.
24. C. Ortega, A. Arias, C. Caruana, J. Balcells, M. Asher, Improved Waveform Quality in the Direct Torque Control of Matrix-Converter-Fed PMSM Drives, IEEE transaction on Industrial Electronics 57 (2010) 2101-2110.

Table A.1. Switching States for 3-phase to 5-phase matrix converter (large vectors in $d-q$ and small vectors in z_1-z_2)

State	a	b	c	d	e	$\lvert V_o^{d-q}\rvert$	α_o^{d-q}	$\lvert V_o^{z_1-z_2}\rvert$	$\lvert\alpha_o^{z_1-z_2}\rvert$
1	A	A	A	B	B	0.647|VAB|	72°	0.247|VAB|	36°
2	A	A	A	C	C	0.647|VAC|	72°	0.247|VAC|	36°
3	A	A	B	B	A	0.647|VAB|	0°	0.247|VBA|	0°
4	A	A	B	B	B	0.647|VAB|	36°	0.247|VAB|	-72°
5	A	A	C	C	A	0.647|VAC|	0°	0.247|VCA|	0°
6	A	A	C	C	C	0.647|VAC|	36°	0.247|VAC|	-72°
7	A	B	B	A	A	0.647|VAB|	-72°	0.247|VAB|	-36°
8	A	B	B	B	A	0.647|VAB|	-36°	0.247|VAB|	72°
9	A	C	C	A	A	0.647|VAC|	-72°	0.247|VAC|	-36°
10	A	C	C	C	A	0.647|VAC|	-36°	0.247|VAC|	72°
11	B	B	B	A	A	0.647|VBA|	72°	0.247|VBA|	36°
12	B	B	B	C	C	0.647|VBC|	72°	0.247|VBC|	36°
13	B	B	A	A	B	0.647|VBA|	0°	0.247|VAB|	0°
14	B	B	A	A	A	0.647|VBA|	36°	0.247|VBA|	-72°
15	B	B	C	C	B	0.647|VBC|	0°	0.247|VCB|	0°
16	B	B	C	C	C	0.647|VBC|	36°	0.247|VBC|	-72°
17	B	A	A	B	B	0.647|VBA|	-72°	0.247|VBA|	-36°
18	B	A	A	A	B	0.647|VBA|	-36°	0.247|VBA|	72°
19	B	C	C	B	B	0.647|VBC|	-72°	0.247|VBC|	-36°
20	B	C	C	C	B	0.647|VBC|	-36°	0.247|VBC|	72°
21	C	C	C	B	B	0.647|VCB|	72°	0.247|VCB|	36°
22	C	C	C	A	A	0.647|VCA|	72°	0.247|VCA|	36°
23	C	C	B	B	C	0.647|VCB|	0°	0.247|VBC|	0°
24	C	C	B	B	B	0.647|VCB|	36°	0.247|VCB|	-72°
25	C	C	A	A	C	0.647|VCA|	0°	0.247|VAC|	0°
26	C	C	A	A	A	0.647|VCA|	36°	0.247|VCA|	-72°
27	C	B	B	C	C	0.647|VCB|	-72°	0.247|VCB|	-36°
28	C	B	B	B	C	0.647|VCB|	-36°	0.247|VCB|	72°
29	C	A	A	C	C	0.647|VCA|	-72°	0.247|VCA|	-36°
30	C	A	A	A	C	0.647|VCA|	-36°	0.247|VCA|	72°

Table A.2. Switching States for 3-phase to 5-phase matrix converter (medium vectors in $d-q$ and medium vectors in z_1-z_2)

State	a	b	c	d	e	$\lvert V_o^{d-q}\rvert$	α_o^{d-q}	$\lvert V_o^{z_1-z_2}\rvert$	$\lvert\alpha_o^{z_1-z_2}\rvert$
31	A	A	A	A	B	0.4|VBA|	-72 °	0.4|VAB|	-36 °
32	A	A	A	A	C	0.4|VCA|	-72 °	0.4|VAC|	-36 °
33	A	A	A	B	A	0.4|VAB|	36 °	0.4|VBA|	-72 °
34	A	A	A	C	A	0.4|VAC|	36 °	0.4|VCA|	-72 °
35	A	A	B	A	A	0.4|VAB|	-36 °	0.4|VBA|	72 °
36	A	A	C	A	A	0.4|VAC|	-36 °	0.4|VCA|	72 °
37	A	B	A	A	A	0.4|VBA|	72 °	0.4|VAB|	36 °
38	A	B	B	B	B	0.4|VAB|	0 °	0.4|VAB|	0 °
39	A	C	A	A	A	0.4|VCA|	72 °	0.4|VAC|	36 °
40	A	C	C	C	C	0.4|VAC|	0 °	0.4|VAC|	0 °
41	B	B	B	B	A	0.4|VAB|	-72 °	0.4|VBA|	-36 °
42	B	B	B	B	C	0.4|VCB|	-72 °	0.4|VBC|	-36 °
43	B	B	B	A	B	0.4|VBA|	36 °	0.4|VAB|	-72 °
44	B	B	B	C	B	0.4|VBC|	36 °	0.4|VCB|	-72 °
45	B	B	A	B	B	0.4|VBA|	-36 °	0.4|VAB|	72 °
46	B	B	C	B	B	0.4|VBC|	-36 °	0.4|VCB|	72 °
47	B	A	B	B	B	0.4|VAB|	72 °	0.4|VBA|	36 °
48	B	A	A	A	A	0.4|VBA|	0 °	0.4|VBA|	0 °
49	B	C	B	B	B	0.4|VCB|	72 °	0.4|VBC|	36 °
50	B	C	C	C	C	0.4|VBC|	0 °	0.4|VBC|	0 °
51	C	C	C	C	B	0.4|VBC|	-72 °	0.4|VCB|	-36 °
52	C	C	C	C	A	0.4|VAC|	-72 °	0.4|VCA|	-36 °
53	C	C	C	B	C	0.4|VCB|	36 °	0.4|VBC|	-72 °
54	C	C	C	A	C	0.4|VCA|	36 °	0.4|VAC|	-72 °
55	C	C	B	C	C	0.4|VCB|	-36 °	0.4|VBC|	72 °
56	C	C	A	C	C	0.4|VCA|	-36 °	0.4|VAC|	72 °
57	C	B	C	C	C	0.4|VBC|	72 °	0.4|VCB|	36 °
58	C	B	B	B	B	0.4|VCB|	0 °	0.4|VCB|	0 °
59	C	A	C	C	C	0.4|VAC|	72 °	0.4|VCA|	36 °
60	C	A	A	A	A	0.4|VCA|	0 °	0.4|VCA|	0 °

Table A.3. Switching States for 3-phase to 5-phase matrix converter (small vectors in $d-q$ and large vectors in z_1-z_2)

State	a	b	c	d	e	$\lvert V_o^{d-q}\rvert$	α_o^{d-q}	$\lvert V_o^{z_1-z_2}\rvert$	$\lvert\alpha_o^{z_1-z_2}\rvert$
61	A	A	B	A	B	0.247|VAB|	36 °	0.647|VAB|	-72 °
62	A	A	C	A	C	0.247|VAC|	36 °	0.647|VAC|	-72 °
63	A	B	A	A	B	0.247|VBA|	0 °	0.647|VAB|	0 °
64	A	B	A	B	B	0.247|VAB|	72 °	0.647|VAB|	36 °
65	A	B	A	B	A	0.247|VAB|	-36 °	0.647|VAB|	72 °
66	A	B	B	A	B	0.247|VAB|	-72 °	0.647|VAB|	-36 °
67	A	C	A	A	C	0.247|VCA|	0 °	0.647|VAC|	0 °
68	A	C	A	C	A	0.247|VAC|	-36 °	0.647|VAC|	72 °
69	A	C	A	C	C	0.247|VAC|	72 °	0.647|VAC|	36 °
70	A	C	C	A	C	0.247|VAC|	-72 °	0.647|VAC|	-36 °
71	B	B	A	B	A	0.247|VBA|	36 °	0.647|VBA|	-72 °
72	B	B	C	B	C	0.247|VBC|	36 °	0.647|VBC|	-72 °

73	B	A	B	B	A	0.247|VAB|	0 °	0.647|VBA|	0 °
74	B	A	B	A	A	0.247|VBA|	72 °	0.647|VBA|	36 °
75	B	A	B	A	B	0.247|VBA|	-36 °	0.647|VBA|	72 °
76	B	A	A	B	A	0.247|VBA|	-72 °	0.647|VBA|	-36 °
77	B	C	B	B	C	0.247|VCB|	0 °	0.647|VBC|	0 °
78	B	C	B	C	B	0.247|VBC|	-36 °	0.647|VBC|	72 °
79	B	C	B	C	C	0.247|VBC|	72 °	0.647|VBC|	36 °
80	B	C	C	B	C	0.247|VBC|	-72 °	0.647|VBC|	-36 °
81	C	C	B	C	B	0.247|VCB|	36 °	0.647|VCB|	-72 °
82	C	C	A	C	A	0.247|VCA|	36 °	0.647|VCA|	-72 °
83	C	B	C	C	B	0.247|VBC|	0 °	0.647|VCB|	0 °
84	C	B	C	B	B	0.247|VCB|	72 °	0.647|VCB|	36 °
85	C	B	C	B	C	0.247|VCB|	-36 °	0.647|VCB|	72 °
86	C	B	B	C	B	0.247|VCB|	-72 °	0.647|VCB|	-36 °
87	C	A	C	C	A	0.247|VAC|	0 °	0.647|VCA|	0 °
88	C	A	C	A	C	0.247|VCA|	-36 °	0.647|VCA|	72 °
89	C	A	C	A	A	0.247|VCA|	72 °	0.647|VCA|	36 °
90	C	A	A	C	A	0.247|VCA|	-72 °	0.647|VCA|	-36 °